

Order–Disorder of the Hydronium Ion and Low-Temperature Phase Transition of $(\text{H}_3\text{O})\text{Zr}_2(\text{PO}_4)_3$ NASICON by Neutron Diffraction

Michele Catti*

Dipartimento di Scienza dei Materiali, Università di Milano Bicocca, via Cozzi 53, 20125 Milano, Italy

Richard M. Ibberson

ISIS Facility, CCLRC Rutherford Appleton Laboratory, Chilton, Didcot, Oxon, OX11 0QX U.K.

Received: June 13, 2002

High-resolution powder neutron diffraction data (HRPD, ISIS Facility, U.K.) were collected on $(\text{H}_3\text{O})\text{Zr}_2(\text{PO}_4)_3$ between 4 and 300 K. In the range 175–180 K, a ferroelastic first-order phase transition from the rhombohedral $R\bar{3}c$ NASICON structure to a monoclinic distorted one was discovered. Rietveld structure refinements were performed at 300 K ($a = 8.74848(3)$, $c = 23.7598(1)$ Å) and 4.5 K (space group $C2/c$ or Cc , $a = 15.0663(1)$, $b = 8.7878(1)$, $c = 9.3611(1)$ Å, $\beta = 122.498(1)^\circ$). At RT, the hydronium ion H_3O^+ is pyramidal disordered over two inversion-related configurations. At LT, H_3O^+ becomes nearly planar, with two H atoms ordered and hydrogen-bonded to neighboring oxygens, and the third H atom disordered over two close positions with 2/3 and 1/3 statistical occupancies. Relations with the structural features of hydronium in other structures and the nature of order–disorder are discussed. An atomistic mechanism for proton conductivity is proposed.

1. Introduction

NASICON-type compounds are important materials for solid-state ionic conductivity; they can show a quite variable chemical composition summarized as $\text{A}_x\text{M}_2(\text{XO}_4)_3$, where X (P, S, and Si) has tetrahedral oxygen coordination, M is a (mostly transition) metal atom octahedrally coordinated, and A is usually a monovalent cation.¹ The NASICON structure, rhombohedral $R\bar{3}c$, can be derived from that of corundum Al_2O_3 by substitution of aluminum by M and of oxygen by tetrahedral groups XO_4 .² A three-dimensional network of coordination MO_6 octahedra and XO_4 tetrahedra sharing corners ensues. Large cavities are present around Wyckoff positions 6(b) at 0,0,0 with site symmetry $\bar{3}$ (M' sites), which correspond to the empty octahedral sites in the hexagonal Al layers of corundum, and which are occupied by A^+ cations in NASICON phases. When A is an alkali atom, a large ionic conductivity is very often observed; this has been ascribed to the presence of a number of sites suitable for hosting A^+ cations along the pathway connecting adjacent M' cavities: cf. the cases of $\text{LiZr}_2(\text{PO}_4)_3$ above 50 °C and $\text{Na}_3\text{Zr}_2(\text{SiO}_4)_2\text{PO}_4$ above 170 °C;^{2–4} at RT, such compounds are stable in triclinic $C\bar{1}$ and monoclinic $C2/c$ modifications, respectively.

The H-substituted NASICON was synthesized,⁵ and it was given the formula $(\text{H}_3\text{O})\text{Zr}_2(\text{PO}_4)_3$ on the basis of a powder neutron diffraction study at 15 K which showed the presence of a hydronium ion H_3O^+ on the M' site, with each of the three H atoms disordered over two centrosymmetrical positions.⁶ An appreciable protonic conductivity was measured,^{5,7} raising a number of questions about the detailed mechanisms of proton mobility in hydronium ion compounds. In particular, the claimed extensive disorder of H atoms at 15 K appeared somehow puzzling, and let us suspect that some kind of order–disorder

phase transition should occur, perhaps at even lower temperature. The hypothesis of a transformation related to an umbrella-like inversion of the H_3O^+ pyramid, similarly to NH_3 , seemed to be particularly interesting. We therefore decided to undertake a very careful, high-resolution powder neutron diffraction study of $(\text{H}_3\text{O})\text{Zr}_2(\text{PO}_4)_3$ at variable temperature down to 4 K, to clarify such open questions.

2. Experimental Section

$(\text{H}_3\text{O})\text{Zr}_2(\text{PO}_4)_3$ was prepared by ion exchange of $\text{LiZr}_2(\text{PO}_4)_3$ in 8 N solution of HCl at 80 °C for 4 days. The lithium compound had been synthesized by solid-state reaction of Li_2CO_3 , ZrO_2 , and $\text{NH}_4\text{H}_2\text{PO}_4$ at 1200 °C.^{8,9} X-ray diffractometry (Cu $\text{K}\alpha$ radiation) proved the ion exchange reaction to be complete, with no residual presence of the lithium phase, and confirmed the pattern indexing according to the rhombohedral space group $R\bar{3}c$.

Neutron diffraction data were collected on the time-of-flight high-resolution powder diffractometer (HRPD) at the ISIS spallation pulsed source, Rutherford Appleton Laboratory (U.K.). The 2 cm³ sample was contained in a vanadium can sealed with indium at room pressure, to prevent a possible dehydration under vacuum. Measurements were carried out below room temperature in a liquid He cryostat, and at 300 K without cryostat. All intensity profiles were recorded in the d_{hkl} range 0.69–2.4 Å (4226 data) by use of the backscattering counter bank at $2\theta = 168.3^\circ$, with maximum resolution of $\Delta d/d \approx 4 \times 10^{-4}$. Accurate data for structure refinement (12 h) were collected at 300 and 4.5 K (Figure 1); at intermediate temperatures, shorter times (2 h) were used. Rietveld refinements were carried out by the GSAS computer package.¹⁰ The background intensity was modeled by a Chebyshev polynomial of first kind with 12 coefficients, and the peak shape was modeled by a convolution of a pseudo-Voigt function (linear combination of Gaussian and Lorentzian components, with σ and γ half-widths,

* To whom correspondence should be addressed. E-mail: catti@mater.unimib.it. Fax: +39-02-6448-5400.

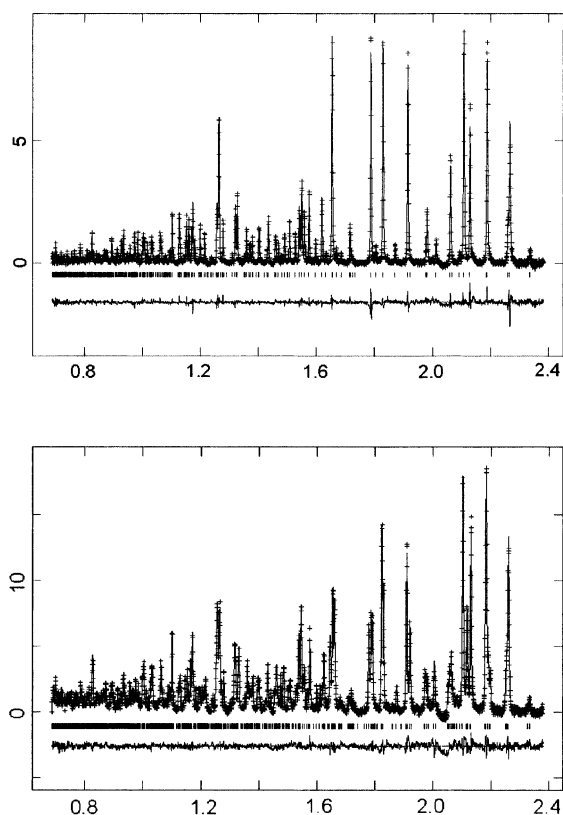


Figure 1. Experimental (crosses), calculated, and difference profiles of the powder neutron diffraction pattern of α -(H₃O)Zr₂(PO₄)₃ (above, T = 300 K) and α'' -(H₃O)Zr₂(PO₄)₃ (below, T = 4.5 K). Counts/time (μs^{-1}) are plotted vs d_{hkl} spacing (Å).

respectively: sample contribution) with two back-to-back exponentials (instrumental and moderator contributions).¹¹ Linear dependences of the σ and γ parameters on d_{hkl} were assumed: $\sigma = \sigma_1 d_{hkl}$, $\gamma = \gamma_1 d_{hkl}$. The mixing coefficient and the full width of the pseudo-Voigt function depend on σ and γ according to equations given in the literature.¹²

3. Results and Discussion

3.1. Phase Transition. The sample of (H₃O)Zr₂(PO₄)₃ was cooled to 4.5 K and then heated by steps till RT, collecting diffraction profiles at a number of intermediate temperatures. All patterns below 180 K appeared to be more complex than that of the rhombohedral NASICON structure (Figure 1), and they could be indexed on the basis of a monoclinic C lattice related to the rhombohedral one by the $[1\bar{1}0 \mid 110 \mid -1/3 \ 1/3 \ 1/3]$ matrix transformation (the rows are components of the monoclinic cell vectors in the hexagonal reference). This relationship is similar to that relating the $R\bar{3}c$ to the $C2/c$ structure of Na₃Zr₂(SiO₄)₂PO₄³ and to the $C\bar{1}$ of LiZr₂(PO₄)₃.² The unit-cell constants were derived by Rietveld refinements, keeping the atomic coordinates fixed at the values refined at 4.5 or 300 K for the monoclinic or rhombohedral phase (see below). The behavior of a , b , and c vs T is shown in Figure 2; values in the rhombohedral stability range have been transformed into the corresponding monoclinic ones according to $a_M = a_H\sqrt{3}$, $b_M = b_H$, $c_M = (3a_H^2 + c_H^2)^{1/2}/3$.

Thus, (H₃O)Zr₂(PO₄)₃ undergoes a phase transition between the rhombohedral α structure and a new monoclinic one, called hereafter α'' , with $175 \text{ K} < T_c < 180 \text{ K}$. This phenomenon was not detected in the previous study,⁶ possibly for insufficient resolution of the experiment. Sharp discontinuities of all cell

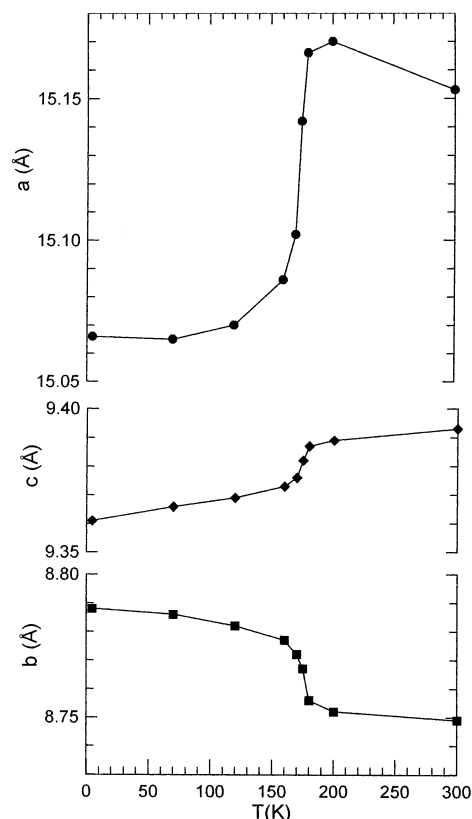


Figure 2. Thermal evolution of the unit-cell edges of (H₃O)Zr₂(PO₄)₃, showing the monoclinic α'' to rhombohedral α phase transition at 177 K. The monoclinic reference frame is used also for the rhombohedral cell.

edges (in particular a) denote clearly a first-order character of the transition. On the other hand, the ferroelastic nature of the rhombohedral to monoclinic lattice distortion, and the symmetry group/subgroup relation between the α ($R\bar{3}c$) and α'' ($C2/c$) structures, would indicate a displacive or order–disorder rather than reconstructive mechanism for the phase transition. This point was fully clarified by the crystal structure determinations at 300 and 4.5 K.

3.2. Room-Temperature Structure. The RT structure (α phase) was Rietveld-refined on the basis of the $R\bar{3}c$ ideal NASICON configuration, with the OW oxygen atom of hydronium on the $\bar{3}$ site at 0,0,0 and H in general position with a fractional occupancy of $1/2$, according to the structural model proposed by Rudolf et al.⁶ and shown in Figure 3. Convergence was attained, with isotropic thermal factors, at $R_p = 0.0240$, $wR_p = 0.0276$ and $R(F^2) = 0.0855$ (Table 1). A peculiar feature of the results is the high U_{iso} value of OW, indicating either a real large thermal motion of the whole hydronium ion inside the M' cavity of the NASICON framework or possibly the preference of OW for a position slightly displaced from the 3-fold axis with a locally lowered symmetry. To detect the largest components of the OW atomic displacement, the structure was refined with anisotropic thermal factors for all atoms but H, yielding $U_{11} = U_{22} = 7.6(2)$ and $U_{33} = 3.9(3) \times 10^{-2} \text{ Å}^2$; thus, a preferential displacement of OW within the (001) plane is observed. An isotropic refinement was then attempted with OW slightly off the $\bar{3}$ site and fractional occupancy $1/6$. Convergence was obtained with a marginal improvement of the above R indexes, and with a shift of 0.31 Å of OW from the high symmetry site, which is hardly larger than the square root of U_{11} ; $U_{iso}(OW)$ lowered to $3.0(8) \times 10^{-2} \text{ Å}^2$. The esd's of atomic coordinates and interatomic distances

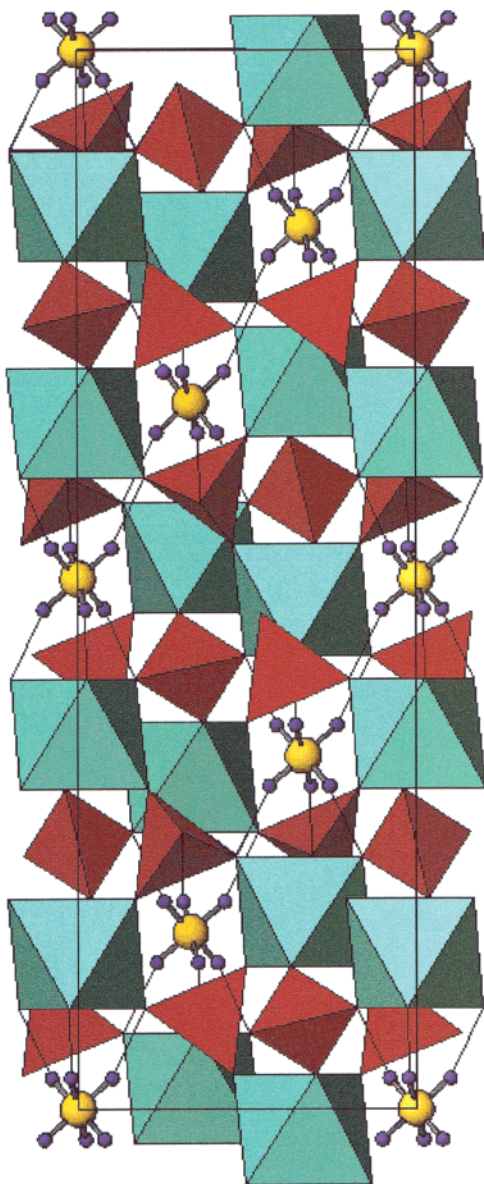


Figure 3. Crystal structure of α -(H_3O) $\text{Zr}_2(\text{PO}_4)_3$ at room temperature, projected onto the (1 2 0) plane and emphasizing the PO_4 and ZrO_6 coordination polyhedra. The disordered hydronium ions with pyramidal configuration, and their hydrogen bonding system, are shown.

increase substantially, and the environment of the OW atom becomes qualitatively similar to that shown in the low-temperature $C2/c$ or Cc structure (cf. below). We conclude that the local structure of α -(H_3O) $\text{Zr}_2(\text{PO}_4)_3$ has probably a lower symmetry than $R\bar{3}c$, possibly monoclinic similarly to the LT phase, though within a geometrically rhombohedral lattice; the RT phase would be a small-scale domain-like pattern simulating, on the average, the rhombohedral structure. On the basis of the resolution presently available for the best powder diffraction experiments, however, it is not possible to refine accurately this structural model. To investigate the dynamic motion of hydronium between the six close sites related by the $\bar{3}$ symmetry, quasielastic neutron spectroscopy experiments are under way.

3.3. Low-Temperature Structure. At first, the $C2/c$ structure of $\text{Na}_3\text{Zr}_2(\text{SiO}_4)_2\text{PO}_4$ (without the alkaline metal atom) was assumed as trial structural model,³ excluding the hydronium ion, for the α'' phase at 4.5 K. A similar configuration is also shown by α' - $\text{LiZr}_2(\text{PO}_4)_3$ (triclinic $C\bar{1}$).⁸ The atomic coordinates of the

TABLE 1: Atomic Occupation Factors, Fractional Coordinates, and Thermal Parameters of the Rhombohedral α ($R\bar{3}c$, $Z = 6$, $T = 300$ K) and Monoclinic α'' ($C2/c$, $Z = 4$, $T = 4.5$ K) Phases of (H_3O) $\text{Zr}_2(\text{PO}_4)_3$ ^a

	o.f.	x	y	z	U_{iso}
α phase					
Zr	1	0	0	0.14956(7)	0.99(3)
P	1	0.2863(2)	0	0.25	1.14(4)
O1	1	0.1694(2)	-0.0380(2)	0.19862(5)	2.30(3)
O2	1	0.1986(2)	0.1728(1)	0.09497(5)	2.05(4)
OW	1	0	0	0	6.6(1)
H	0.5	-0.0221(8)	-0.1004(8)	0.0288(2)	6.3(2)
α'' phase					
Zr	1	0.3991(2)	0.2484(3)	0.4491(3)	0.37(4)
P1	1	0.1464(2)	0.0992(3)	0.2583(4)	0.41(6)
P2	1	0	0.5308(4)	0.25	0.02(2)
O1	1	0.5484(3)	0.3255(3)	0.6088(4)	0.73(7)
O2	1	0.3486(2)	0.3778(3)	0.5761(4)	0.72(7)
O3	1	0.4205(2)	0.0692(3)	0.6029(4)	0.72(8)
O4	1	0.3560(2)	0.4275(3)	0.2745(4)	0.86(7)
O5	1	0.2441(3)	0.1709(3)	0.2713(4)	0.74(7)
O6	1	0.4436(3)	0.1303(4)	0.3097(4)	1.19(9)
OW	0.5	0.2240(6)	0.2399(12)	-0.0014(12)	2.2(2)
H1	0.5	0.2005(8)	0.1703(12)	-0.0997(14)	2.2(3)
H2	0.5	0.2331(9)	0.2125(13)	0.1049(14)	2.7(3)
H3	0.33(2)	0.2657(17)	0.3159(22)	-0.0058(29)	1.6(4)
H3''	0.17(2)	0.2066(32)	0.3429(25)	-0.0430(45)	2.8(9)

^a The lattice constants are $a = 8.74848(3)$, $c = 23.7598(1)$ Å (α), and $a = 15.0663(1)$, $b = 8.7878(1)$, $c = 9.3611(1)$ Å, $\beta = 122.498(1)^\circ$ (α''). Units of U_{iso} are 10^{-2} Å². The esd's are reported in parentheses.

monoclinic and rhombohedral structures are related by the transformation:

$$x_{\text{M}} = (x_{\text{H}} - y_{\text{H}})/2 + z_{\text{H}} + 1/4; \quad y_{\text{M}} = (x_{\text{H}} + y_{\text{H}})/2 + 1/4; \\ z_{\text{M}} = 3z_{\text{H}}$$

A difference Fourier map revealed immediately the hydronium oxygen atom OW disordered over two centrosymmetrical positions close to the inversion center at $1/4 \ 1/4 \ 0$ and the H1 and H2 hydrogen atoms bonded to OW and hydrogen-bonded to the O4 and O5 oxygen atoms of neighboring phosphate groups. Then, after least-squares refinement, a subsequent difference map showed two further negative peaks close to OW, which could be interpreted as alternative positions of the third missing hydrogen atom. Thus, two further H atoms were included in the refinement, with their o.f.'s constrained to sum to 0.5. The occupancies and thermal factors of H3 and H3'' were refined alternatively till convergence: the H3 position turned out to be definitely more populated than the other one, with a ratio 2:1. As the distances of H3 and H3'' to OW were slightly short (about 0.90 Å), a soft constraint was introduced in the refinement, corresponding to a O-H distance of 0.96 Å. The final isotropic cycle converged to $R_{\text{p}} = 0.0130$, $wR_{\text{p}} = 0.0156$, and $R(F^2) = 0.0580$, and the refined parameters are reported in Table 1.

The disorder of the whole hydronium ion over two close centrosymmetrically related sites in the $C2/c$ structure of (H_3O) $\text{Zr}_2(\text{PO}_4)_3$ raises some problems. Clearly, at 4.5 K, a static rather than dynamical character of the disorder is more likely. Therefore, the $C2/c$ structural model implies a domain structure with the hydronium ion locally ordered in one of two equivalent positions slightly off the center of symmetry at $1/4 \ 1/4 \ 0$. Each one of the two configurations corresponds to either enantiomorph of a noncentrosymmetrical structural model whose space group must be a subgroup of $C2/c$. Out of the three possibilities Cc , $C2$, and $C1$, the complex triclinic case $C1$ was excluded. A

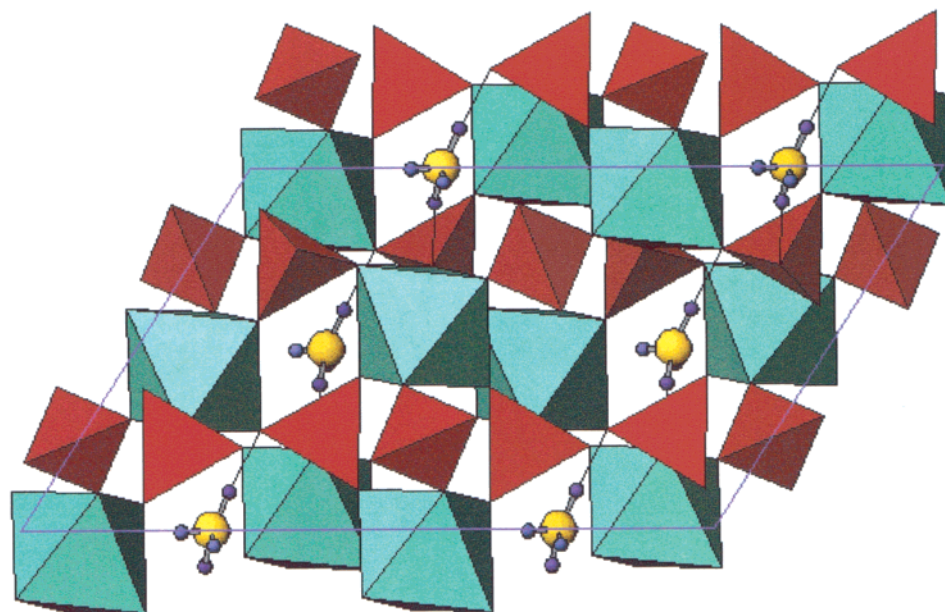


Figure 4. Crystal structure of α'' -(H₃O)Zr₂(PO₄)₃ at 4.5 K, projected onto the (0 1 0) plane. The hydronium ion has a nearly planar configuration, with ordered H1 (below) and H2 (above) atoms, and a statistical occupancy of H3 (left) and H3'' (right).

structural refinement in space group *C2* did not converge, whereas convergence could be attained in *Cc*, with the hydronium atoms OW, H1, H2, H3, and H3'' ordered in one of the two centrosymmetrical positions of the *C2/c* model. All other atoms of the asymmetric unit but P2 are related in pairs by pseudocentrosymmetry. A residual disorder, unrelated to symmetry, remains for the third hydronium H atom distributed between the H3 and H3'' sites, with occupation factors of 2/3 and 1/3 corresponding to the results of the *C2/c* refinement.

By comparison with the results of the *C2/c* refinement, it can be noticed that (i) the improvement of agreement factors is hardly significant; (ii) the esd's of atomic coordinates and bond distances increase substantially; (iii) PO₄ tetrahedra become more distorted; (iv) the only significant structural changes are the lengthening of the two hydrogen bridges from 2.48 and 2.62 Å to 2.56 and 2.67 Å, respectively, and the decrease of the H1—OW—H2 angle from 126 to 117°. The other geometrical features of the hydronium ion do not vary substantially. We conclude that the real structure of monoclinic α'' -(H₃O)Zr₂(PO₄)₃ corresponds very likely to the acentric *Cc* model, which however cannot be refined accurately because of the large number of parameters and the strong correlations due to pseudocentrosymmetry. That model is quite similar to the locally ordered *C2/c* structure, obtained by removing one of the two centrosymmetrically related hydronium ions (Figure 4).

In Table 2, the P—O and Zr—O interatomic distances are reported for the two polymorphs of (H₃O)Zr₂(PO₄)₃. A slight increase of distortion of both the PO₄ tetrahedra and ZrO₆ octahedra is observed in the LT α'' with respect to the RT α phase.

3.4. Hydronium Ion. In the RT α phase, the average structure of the hydronium ion, with OW at 0,0,0 surrounded by six disordered H half-atoms at 1.052 Å (Table 3, Figures 3 and 5, left), can be interpreted on the basis of two kinds of locally ordered configurations with pyramidal shapes. The first one has the three H atoms pointing either upward or downward along the *c* axis, with H—OW—H angles of 98°. The second possible local configuration shows two H pointing upward and one downward, or vice-versa, with two H—OW—H angles of 82° and one of 98°. All H atoms are linked, by fairly long hydrogen

TABLE 2: P—O and Zr—O Interatomic Distances (Å) in α -(H₃O)Zr₂(PO₄)₃ (R3c, *T* = 300 K) and α'' -(H₃O)Zr₂(PO₄)₃ (C2/c, *T* = 4.5 K)^a

α phase			
P—O1	1.519(2) × 2	Zr—O1	2.039(2) × 3
O2	1.531(2) × 2	O2	2.088(2) × 3
<P—O>	1.525	<Zr—O>	2.064
α'' phase			
P1—O1	1.535(5)	Zr—O1	2.034(5)
O2	1.524(4)	O2	2.063(5)
O4	1.537(4)	O3	2.039(5)
O5	1.544(5)	O4	2.104(4)
<P1—O>	1.535	O5	2.125(5)
		O6	2.043(5)
P2—O3	1.527(4) × 2	<Zr—O>	2.068
O6	1.519(4) × 2		
<P2—O>	1.523		

^a The esd's are reported in parentheses.

TABLE 3: Interatomic Distances (Å) and Angles (deg) of the Hydronium Ion H₃O⁺ in Rhombohedral α (*T* = 300 K, above) and Monoclinic α'' (*T* = 4.5 K, below) (H₃O)Zr₂(PO₄)₃^a

OW—H	1.052(6) × 6	∠H—OW—H	97.7(4) × 6 82.3(4) × 6
OW—O2	2.787(1)		
H—O2	1.784(6)	∠OW—H—O2	157.9(4)
OW—H1	1.00(1)	∠H1—OW—H2	126(1)
H2	0.96(1)	∠H1—OW—H3	108(2)
H3	0.93(2)	∠H2—OW—H3	120(2)
H3''	0.97(2)	∠H1—OW—H3''	109(2)
OW—O4	2.615(11)	∠H2—OW—H3''	121(2)
O5	2.480(10)	∠H3—OW—H3''	36(2)
H1—O4	1.626(11)	∠OW—H1—O4	171(1)
H2—O5	1.520(12)	∠OW—H2—O5	178(1)

^a The esd's are reported in parentheses.

bridges (with correspondingly quite bent OW—H—O angles), to oxygens at the corners of triangular faces of the ZrO₆ octahedra lying above and below the hydronium ion.

In the LT monoclinic structure, the hydronium ion has two ordered H atoms (H1 and H2) hydrogen-bonded to neighboring oxygens of PO₄ groups and a third not hydrogen-bonded H atom disordered over two close positions (H3 and H3''); these are

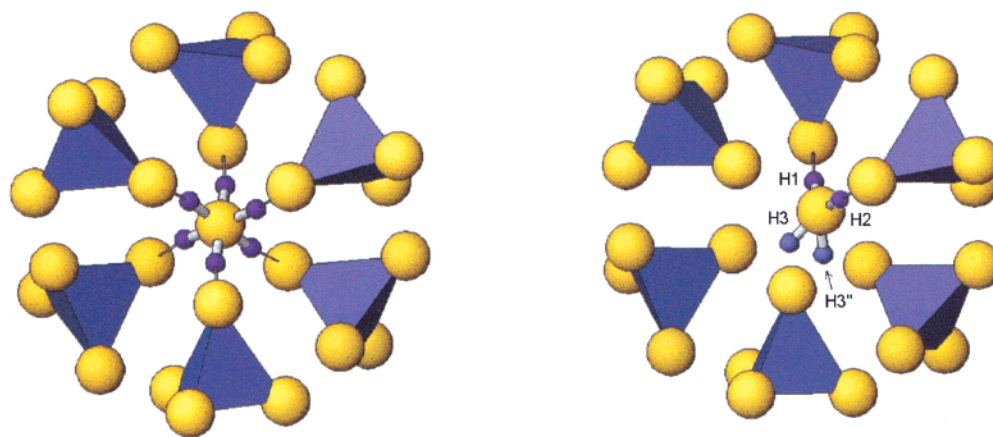


Figure 5. Configuration and surrounding of the disordered hydronium ion H_3O^+ in the RT rhombohedral α (left) and LT monoclinic α'' (right) phases of $(\text{H}_3\text{O})\text{Zr}_2(\text{PO}_4)_3$. Projection onto the (001) plane, showing PO_4 tetrahedra and hydrogen bonds (thin rods). The occupancy of all H atoms is 0.5 in the left structure; in the right one, H1 and H2 have full occupancy, and H3 and H3'' have 0.66 and 0.34, respectively.

unrelated by symmetry and lie on either side of the OW–H1–H2 plane (Figures 4 and 5, right). The first configuration of the H_3O^+ ion (OW, H1, H2, H3) has a double statistical population with respect to the second one (OW, H1, H2, H3''), according to the occupation factors of H3 and H3'' (Table 1). A quantum-mechanical tunneling may dynamically relate the H3 and H3'' proton sites, in view of their short spacing of 0.80 Å. Both hydronium ion configurations are geometrically very similar, showing a flat, nearly planar shape of H_3O^+ , with the three H–OW–H angles ranging from 108° to 126°, at variance with the pyramidal geometry observed in the RT phase.

This quite flat geometry of the hydronium ion is consistent with an sp^2 -type hybridization of the OW orbitals and should be compared to other results obtained by neutron diffraction on H_3O^+ -containing crystals. Two recent ND studies on deuterated zeolites (HSAPO-34¹³ and zeolite X¹⁴) will be considered in this respect. In the first one, O–D distances are 0.91, 0.95, and 1.14 Å and D–O–D angles 99, 127, and 130°. The second D_3O^+ ion is constrained by 3-fold axis symmetry, similarly to what happens in $(\text{H}_3\text{O})\text{Zr}_2(\text{PO}_4)_3$ at room temperature; O–D is 1.13 Å, and D–O–D is 88°. Such configurations resemble closely those found in the LT and RT structures of $(\text{H}_3\text{O})\text{Zr}_2(\text{PO}_4)_3$, respectively. It seems therefore to be confirmed that the hydronium ion has two possible configurations: the first is flat, nearly planar, and is typical of ions unconstrained by symmetry; the second one approaches a pyramid with right angles and is observed for ions lying on a 3-fold symmetry axis. As a most important consequence, the possible umbrella-like inversion of the pyramidal hydronium ion is clearly supported. Indeed a flat configuration of H_3O^+ , which would be the nonequilibrium intermediate stage of the process, appears to be stable by itself in definite crystal-chemical environments, so that the activation barrier for inversion could be moderate and the process be favored.

3.5. Proton Mobility. The traditional classification of H^+ transport mechanisms in solid-state proton conductors is based on the four models of classical hopping by thermal activation, quantum-mechanical tunneling, hydrogen bonding (Grotthus-type), and vehicular diffusion.^{15,16} In the present case of $(\text{H}_3\text{O})\text{Zr}_2(\text{PO}_4)_3$ NASICON, taking also into account the results of this structural study, the last mechanism can be surely discarded. A vehicular mobility involves the diffusion-like transport of a whole H_2O or H_3O^+ unit, which usually occurs where large channels or wide interlayer regions are present in the structure, and this is not the case for NASICON. Further, there is no indication of secondary sites for the location of OW,

in addition to the M' one, on our difference Fourier maps. All other mechanisms are possible, taking into account that Grotthus-type processes cannot involve here water-to-water hydrogen bonding because hydronium ions are too far apart.

As different hydronium ions are widely separated in $(\text{H}_3\text{O})\text{Zr}_2(\text{PO}_4)_3$, any mobility pathway of protons under an external electric field must involve intermediate nonequilibrium steps with H^+ bonded to O atoms shared by PO_4 and ZrO_6 groups. In both the α and α'' phases, this can be accomplished only by a proton transfer from the H_3O^+ ion to one of the O acceptors of hydrogen bonds (Grotthus-type first step), according to $\text{H}_2\text{OH}^+ - \text{O}(\text{PO}_3)(\text{ZrO}_5) \rightarrow \text{H}_2\text{O} + \text{H}^+\text{O}(\text{PO}_3)(\text{ZrO}_5)$. Then, a subsequent jump of the proton to a neighboring O atom, belonging to the same PO_4 but to a different ZrO_6 group, is required (second step): $\text{H}^+\text{O}(\text{PO}_3)(\text{ZrO}_5) \rightarrow \text{H}^+\text{O}'(\text{PO}_3)(\text{ZrO}_5)$. Eventually, the proton can hop onto a H_2O molecule formed by another hydronium ion in an adjacent cavity having lost one of its H^+ (Grotthus-type third step: reverse of first step but on a different hydronium). The second step corresponds to a proton jump along the edge of a PO_4 tetrahedron, between sites spaced by about 2.4 Å. It is thus a thermally activated process rather than a tunneling, and should be the rate-determining step of the overall mechanism. This shows some similarities with the proton mobility mechanism proposed for $\text{HTaWO}_6 \cdot \text{H}_2\text{O}$ pyrochlore on the basis of potential energy maps calculations.¹⁷ In that case, however, no hydronium ions are present, and the slow, thermally activated step involves a proton jump along the longer edge of a Ta(W) coordination octahedron.

4. Conclusion

Hydrogenated NASICON $(\text{H}_3\text{O})\text{Zr}_2(\text{PO}_4)_3$, a material of interest for solid-state proton conductivity, has been studied by high-resolution powder neutron diffraction from room-temperature down to 4.5 K. A rhombohedral-to-monoclinic structural transition has been discovered at about 177 K, at variance with previous literature results. This transition corresponds to an ordering of the hydronium ion H_3O^+ and to a change of its configuration from pyramidal to flat. One of the three H atoms is statistically distributed over two sites, probably linked by a proton tunneling dynamics, in the low-temperature phase. The hydrogen bonding system of H_3O^+ should be the basis for a plausible Grotthus-type mechanism of proton mobility in the crystal, with an intermediate step involving a thermally activated proton hopping between O atoms of the same PO_4 tetrahedron.

Acknowledgment. We thank N. Morgante and S. Di Blas for help with the preparation of the sample. This work was supported by grants of M.I.U.R., Roma.

References and Notes

- (1) Alamo, J. *Solid State Ionics* **1993**, 63, 547.
- (2) Catti, M.; Stramare, S. *Solid State Ionics* **2000**, 136–137, 489.
- (3) Boilot, J. P.; Collin, G.; Colomban, Ph. *Mater. Res. Bull.* **1987**, 22, 669.
- (4) Boilot, J. P.; Collin, G.; Colomban, Ph. *J. Solid State Chem.* **1988**, 73, 160.
- (5) Subramanian, M. A.; Roberts, B. D.; Clearfield, A. *Mater. Res. Bull.* **1984**, 19, 1471.
- (6) Rudolf, P. R.; Subramanian, M. A.; Clearfield, A.; Jorgensen, J. D. *Solid State Ionics* **1985**, 17, 337.
- (7) Ohta, M.; Ono, A.; Okamura, F. P. *J. Mater. Sci. Lett.* **1987**, 6, 583.
- (8) Catti, M.; Stramare, S.; Ibberson, R. M. *Solid State Ionics* **1999**, 123, 173.
- (9) Sudreau, F.; Petit, D.; Boilot, J. P. *J. Solid State Chem.* **1989**, 83, 78.
- (10) Larson, A.C.; Von Dreele, R. B. *GSAS: Generalized Structure Analysis System*. Report No. LA-UR 86-748; Los Alamos National Laboratory: Los Alamos, NM, 1994.
- (11) Von Dreele, R. B.; Jorgensen, J. D.; Windsor, C. G. *J. Appl. Crystallogr.* **1982**, 15, 581.
- (12) Thompson, P.; Cox, D. E.; Hastings, J. B. *J. Appl. Crystallogr.* **1987**, 20, 79.
- (13) Smith, L.; Cheetham, A. K.; Morris, R. E.; Marchese, L.; Thomas, J. M.; Wright, P. A.; Chen, J. *Science* **1996**, 271, 799.
- (14) Zhu, L.; Seff, K.; Olson, D. H.; Cohen, B. J.; Von Dreele, R. B. *J. Phys. Chem. B* **1999**, 103, 10365.
- (15) Howe, A. T.; Shilton, M. G. *J. Solid State Chem.* **1979**, 28, 345.
- (16) Kreuer K. D.; Rabenau, A.; Weppner, W. *Angew. Chem.* **1982**, 94, 224.
- (17) Catti, M.; Mari, C. M.; Valerio, G. *J. Solid State Chem.* **1992**, 98, 269.